ANFIS MODELLING, PARTIAL SHADING AND MPPT CONTROLLED HARDWARE ANALYSIS OF STAND ALONE PHOTOVOLTAIC WATER PUMPING SYSTEM

A. Durgadevi[1], S. Arulselvi[2]
Department of Electronics and Instrumentation Engineering
Annamalai University, Chidambaram, Tamil Nadu, India.

Abstract

The solar photovoltaic power has received great attention and experienced impressive progress the countries all over the world in recent years because of more and more serious energy crisis and environmental pollution. Due to scarcity of fossil fuel and increasing demand of power supply, we are forced to utilize the renewable energy resources. Considering easy availability and vast potential, world has turned to solar photovoltaic energy to meet out its ever increasing energy demand. The mathematical modelling and simulation of the photovoltaic system is implemented in the MATLAB/Simulink environment and the same thing is tested and validated using Artificial Intelligent (AI) like ANFIS. This paper proposes an embedded controlled buck converter using PIC 16F877A microcontroller for standalone photovoltaic water pumping application with Incremental conductance algorithm as maximum power point tracker and the same thing is implemented in hardware application till the motor level. The simulated results are matching closely with the hardware results. The output of the controller, pulse generated from PWM can switch MOSFET to change the duty cycle of buck DC-DC converter. The result reveals that the maximum power point is tracked satisfactorily for varying insolation condition. Finally the performance of the photovoltaic array under partially shaded condition is also analysed for varying illumination level.

Key words: Photovoltaic, Pulse Width Modulation, Partial Shading.

I. INTRODUCTION

With the rapid depletion of the conventional fossil fuels, energy crisis and environmental pollution become more and more serious. Today photovoltaic (PV) systems are becoming more and more popular with increase of energy demand and there is also a great environmental pollution around the world due to fossils and oxides. Solar energy which is free and abundant in most parts of world has proven to be economical source of energy in many applications [1]. The energy that the earth receives from the sun is so enormous and so lasting that the total energy consumed annually by the entire world is supplied in as short a time as half an hour. The Photovoltaic panel does not have any moving parts and no materials consumed or emitted. Unfortunately temperature and varying irradiation affects the performance of the photovoltaic system. To overcome this problem, maximum power point tracking technique (MPPT) with incremental conductance as progressing algorithm has been carried out in MATLAB/Simulink environment. The experimentation of the buck converter with integrated incremental conductance maximum power point tracking algorithm has been implemented for standalone photovoltaic water pumping application till the motor level. The discharge rate of the water from the pump with specifications are analyzed theoretically and presented. The proposed over all block diagram of PV system with buck DC-DC converter for water pumping application is shown in Fig.1.

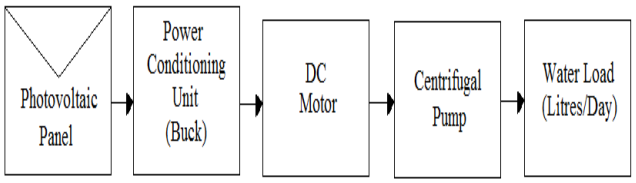

Fig.1. Block diagram of Photovoltaic module with DC-DC buck converter.

2. Mathematical Modeling and ANFIS Validation Of Photovoltaic cell

An equivalent simplified electric circuit of a photovoltaic cell presented in Fig.2.

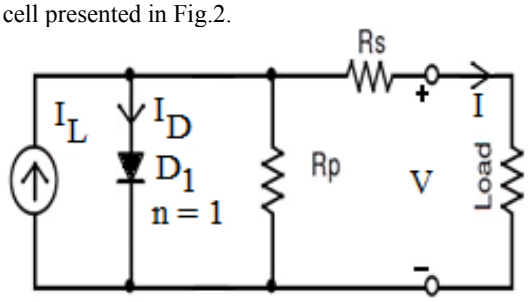

Fig.2. Equivalent circuit of photovoltaic cell.

The expressions obtained from fig.2. are given below.

The load current I_L is obtained is given in equation (1) as,

$$I = I_L - I_o[\exp\left(\frac{q(V+IR_s)}{\gamma k T_c}\right) - 1] \quad (1)$$

I_L is the photo electric current related to the given irradiation condition given by equation (2),

$$I_L = \left(\frac{G}{G_{REF}}\right)\left[I_{L,REF} + \mu_{ISC}\left(T_C - T_{C,REF}\right)\right] \quad (2)$$

The diode saturation current (I_o) is given by the equation (3),

$$I_o = I_{o,REF}\left(\frac{T_C}{T_{C,REF}}\right)^3 \exp\left[\left(\frac{qEg}{k\gamma}\right)\left(\frac{1}{T_{C,REF}} - \frac{1}{T_C}\right)\right] \quad (3)$$

where - I_D is the diode current; I_L- is the photoelectric current related to a given condition of irradiation and temperature; V is the output voltage [V]; I_o is the saturation diode current [A]; γ is the form factor which represents an index of the cell failing; R_s is the series resistance of the cell [Ω]; q is the electric charge ($1.602*10^{-19}$C); k is the Boltzmann's constant ($1.381*10^{-23}$K); T_c is the module temperature [K]. E_g is the energy gap of the material with which the cell is made (for the silicon it is 1.12 eV); G is the radiation [W/m^2]; G_{REF} is the irradiation under standard conditions [W/m^2] $I_{L,REF}$ is the photoelectric current under standard conditions [A]; $T_{C,REF}$ is the module temperature under standard conditions [K]; μ_{ISC} is the temperature coefficient of the short circuit current [A/K], given by the manufacturer according to CEI EN 60891 standard [3-4].

Figure 3 shows the simulated P-V characteristics for varying irradiation and temperature in MATLAB/SIMULINK environment. It can be observed from simulated results as shown in Fig. 3(a), the photo current is directly proportional to irradiation. It is noted from Fig. 3(b) that the terminal voltage increases with decreasing temperature.

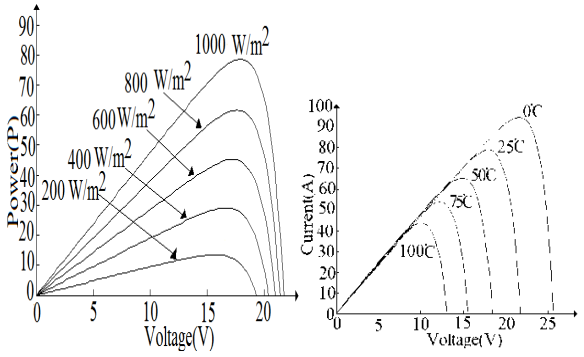

(a) *(b)*

Fig.3. Simulated waveforms showing the effect of (a) radiation and (b) temperature on P-V characteristics.

The manufacturers data at standard conditions are given as P_{max} = 80W, I_{max} = 4.515 A and V_{max} = 21.6V. The simulation results obtained were: P_{max} = 78.51W, I_{max} = 4.35 A and V_{max} = 18.2 V. It is seen that the simulation model showed excellent correspondence to manufacturer's data and therefore this model was considered sufficient for the purpose of further study [4-8].

Simulated I-V, P-V characteristics for the maximum power point tracking (MPPT) is shown in figure.4.

At this Maximum Power Point (MPP), the solar array is matched to its load and when operated at this point the array will yield the maximum power output. From Fig. 4 (a) & (b), it is observed that the power output has an almost linear relationship with array voltage unit, hence the MPP is attained. Any further increase in voltage results in power reduction [5].

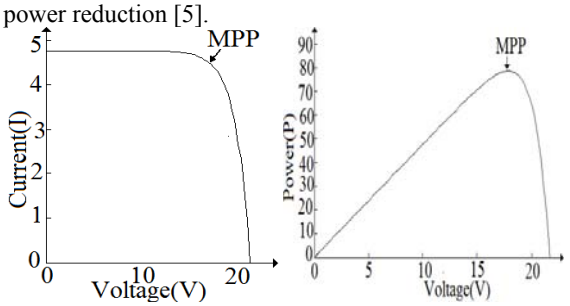

(a) *(b)*

Fig.4. PV array simulated curves (a) I-V curve (25°C) and (b) P-V curve (1000w/m^2).

2.1 ANFIS Modeling of photovoltaic system

The main objective of this work is to investigate the suitability of artificial intelligent systems (neural network and fuzzy logic) for validating the proposed PV system under variable climatic condition. Neural network models are data based where as fuzzy logic models are based on expert knowledge; in a situation in which both data and knowledge of underlying system are available, a neuro fuzzy approach is able to exploit both sources.

Fig.5 shows the simulated result of a photovoltaic power supply system using an adaptive Neuro-Fuzzy Inference System (ANFIS) under standard test condition of irradiation 1000w/m^2 and temperature of 25 °C.

The result reveals that the correlation coefficient between measured values and those estimated by the ANFIS gave good prediction accuracy. The satisfactory performance of ANFIS proves that it can be used for the prediction of the optimal configuration of the PV system.

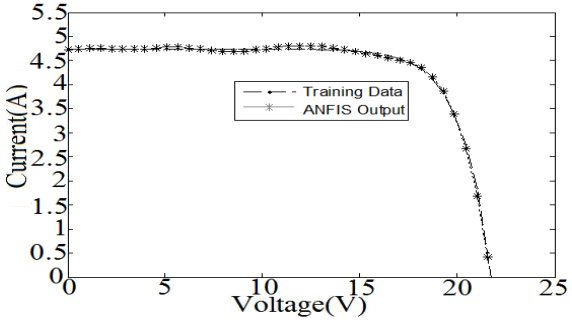

Fig.5. ANFIS modelling of the photovoltaic system for irradiation of 1000w/m^2 and temperature 25 °C.

III. Designing of Buck converter

3.1 Circuit diagram of buck converter.

Fig.6 shows the schematic diagram of buck converter with varying irradiation, which consists of DC supply voltage V_s, as PV generator controlled switch S, diode D, buck inductor L, filter capacitor C and load resistance R.

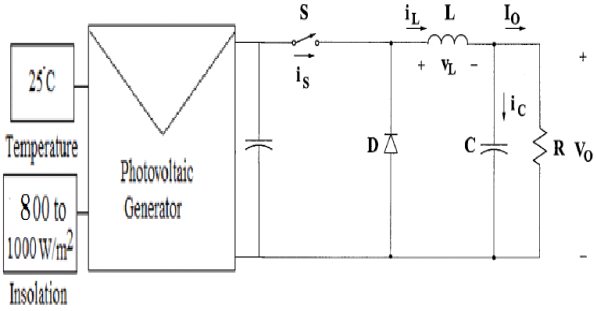

Fig.6. Circuit diagram of buck converter with PV module.

It can be seen from the circuit that when the switch S is commanded to the on state, the Diode D is reverse biased. When the switch S is off, the diode conducts to support an uninterrupted current in the inductor through the output RC circuit using faradays law for the buck inductor as given in (4)

$$(V_s - V_o)DT = (-V_o)(1 - D)T \quad (4)$$

The DC voltage transfer function turns out to be,

$$M_v = \frac{V_o}{V_s} = D \quad (5)$$

The buck converter operates in the CCM for L>Lb. The calculated value of inductance is L=20µH. To limit the ripples in the output side, larger filter capacitor is required. The filter capacitor must provide the output dc current to the load when diode D is off.

The minimum value of filter capacitance calculated that results in the voltage ripple V_r is given by C_{min} =472.5µF. Thus the buck converter is designed in the open loop for the supply voltage of 19.7V DC, which is generated by the Photovoltaic panel for 1000w/m^2 and 25°C.

IV. Closed Loop Simulation of Buck Converter with Incremental Conductance MPPT Algorithm

The block diagram of closed loop simulation with MPPT algorithm is shown in fig.7. To regulate the output voltage V_o, the switching frequency of the PWM pulses are varied depends on error.

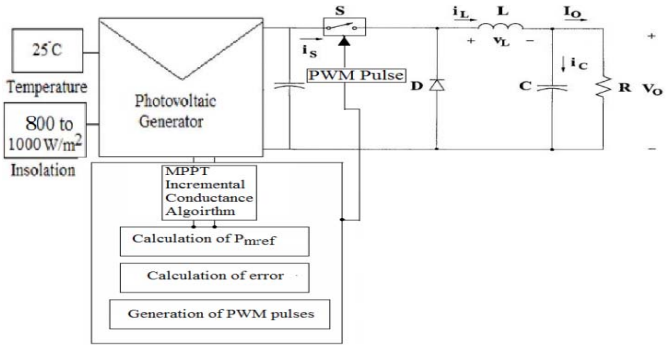

Fig.7. Block diagram of the proposed Incremental Conductance based MPPT scheme.

4.1 MPPT with incremental conductance algorithm

To track and extract maximum power from the PV arrays for a varying insolation level and at a given cell temperature, a conventional controller like proportional integral controller is proposed with incremental conductance algorithm as tracking method [11-16]. The Flow chart of the proposed Incremental Conductance algorithm is shown in Fig.8. This algorithm has the advantage of fast response to the rapidly varying illumination condition. The conventional PI controller parameters are obtained by Z-N open loop method [9] as proportional gain K_c= 1e-5 and integral gain K_i = 0.01.

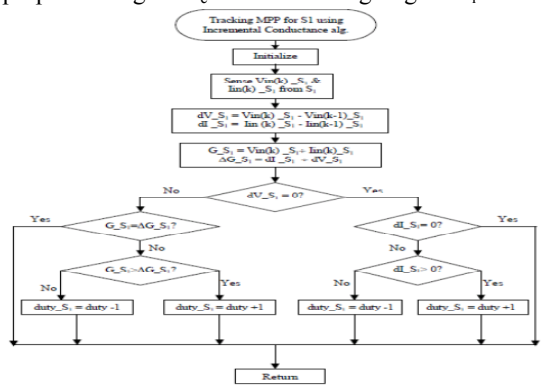

Fig.8. Flow chart of the proposed Incremental Conductance algorithm.

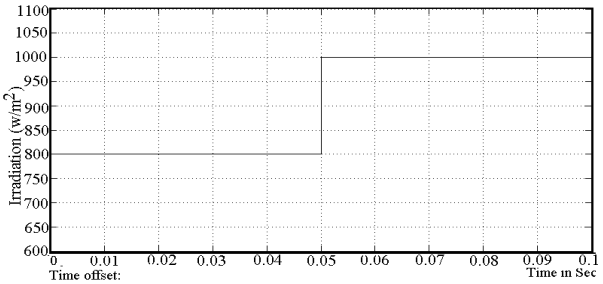

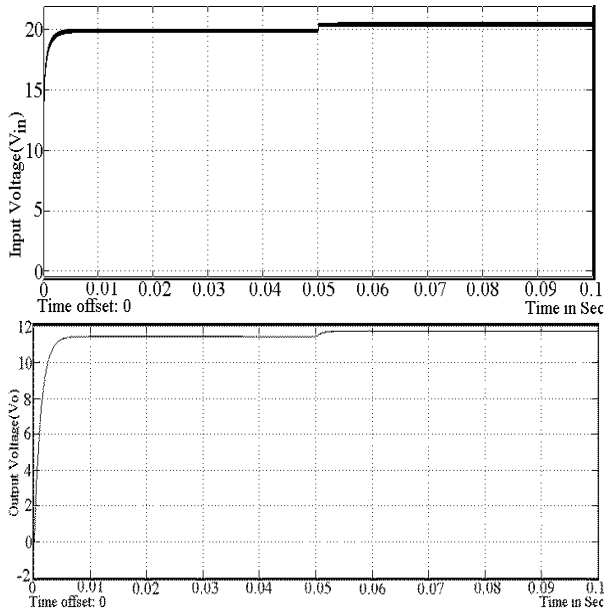

Fig.9. Simulation results depicting the change of insolation from 800 to 1000w/m^2, input voltage (V_{in}) and output voltage (V_o).

The simulated closed loop output for the insolation variation from 800 w/m^2 to 1000 w/m^2 with input voltage (V_{in}) and output voltage (V_o) are shown in Fig.9.

V. Closed Loop Experimental set up

The electrical characteristics of the proposed panel are given in table I.

TABLE I
STANDARD TEST CONDITION DATA

ELECTRICAL CHARACTERISTICS	
Cell	Poly-crystalline silicon
No of cells and connections	36 in series
Open circuit Voltage (V_{oc})	21.75 V
Short – circuit current (I_{sc})	4.85A
Maximum Power Voltage at P_{max} ,(V_{pm})	18.25 V
Maximum Power Current (I_{pm})	4.315 A
Maximum Power (P_{max})	78.24 W (+10%/-5%)
Module Efficiency (ηm)	13%
Series Fuse Rating	10 A
Type of output terminal	Junction Box
Temperature coefficient of I_{sc}	0.65e-3±0.015%/°C
Temperature coefficient of V_{oc}	-160±20mV%/°C
Temperature coefficient of Power	-0.5±0.05%/°C

5.1 Hardware Design

1) Inductor: Inductor losses are hardest to eliminate, because it has a certain number of turns on the coil to maintain the necessary inductance for the converter. The amplitude of the inductor current ripple can be varying between 10% to 20% of its dc value. The maximum converter efficiency appears at the switching frequency of 20 KHz. The calculated value of inductance L=20µH. since, the inductor must at least be able to handle current of 6.5 Amps. Therefore, an inductor of 220µH and its rating of 9.8A chosen for the converter.

2) Output Capacitor: To obtain a desire output voltage ripple, the right value of capacitance is required. Assume that the output voltage ripple is 1% of its dc value (i.e. ΔV_o=0.12V). The minimum value of capacitance value needed for the converter is 472.5µF. hence, a capacitor of 2200µF with 25V is chosen for the design.

3) Diode: diode choice is a tradeoff between breakdown voltage, speed, and forward voltage. The higher forward voltage, the more power that will be dissipated and lost. However, fast diode is needed to act as a switch for the energy in the inductor. If the diode is slow to react, the efficiency of the converter will lower and damaging high voltage transients will develop. In case of these transients and the possibility of large output voltages if the load is suddenly disconnected, the diode also must have a high breakdown voltage. The best combination of these features that could be found was the 1N4007 which has very low forward drop and very high reverse breakdown voltage.

4) Voltage Regulator: since the microcontroller requires a supply voltage of 5V. a step down voltage regulator LM7805 is chosen. Its features are:

- Ultra low quiescent current – Low power consumption, hence it allows a better conversion efficiency of the buck converter.
- 40 V operating voltage limit. It is capable of stepping down the voltage from battery (12V) to 5V.
- Internal short circuit current limits - the microcontroller will be protected if there is a short circuit in the circuitry.
- Internal thermal shutdown protection – this will protect the regulator from over heat if there is a short – in the circuitry.
- Output current up to 1A.
- Safe operating area protection

5) MOSFET: A P channel enhancement mode power MOSFET IRF9540N is used as a high speed switching device for the buck converter. Since the rating of this device is rated at 100V and 23 A, this rating is well above maximum operating voltage and current which are 12V and 6.67A of the converter. It has minimum leakage current of only 100nA and very low on stage resistance of 0.117Ω and hence small conduction loss that makes it a highly efficient switching device.

6) MOSFET Driver: since the PWM current signals generated by the microcontroller can only deliver maximum current of 25mA. It is not suitable to drive a large capacitive load such as a MOSFET, a MOSFET driver MC34152P is used. It has a low output impedance and capable of sourcing and sinking a large

gate current for a short duration. And since it is operating at current as low as 10.5mA and capable of supplying two independent output channels up to 1.5A. This MOSFET driver is a suitable choice since the design required only one PWM signals to switch the power MOSFET.

7) Microcontroller: PIC 16F877A is chosen as a microcontroller for the design. This microcontroller is responsible for all tracker functionality, operating the ADCs and DACs that deal with the analog section, computing what the power point of the array is and monitoring the state of charge of the battery. The PIC16F877A is a perfect combination of features, performance and low power consumption for this application. Its 8K*14 bytes of flash memory, 368*8 bytes of data memory (RAM) two D/A and 8 A/D channel. The one D/A converter pins are used to send the analog voltage (PWMs) back out to set the one DC-DC switching converter to the maximum power point voltage of the PV array. For the 8 A/D converter channels, 2 are used to monitor the PV arrays voltage and current, one is used for monitoring the battery voltage and the final one is reference voltage pin.

8) Voltage divider network: since the PIC16F877A can only process digital information, A/D conversion is required. Analog signals, either the voltage from the voltage divider network or from the differential amplifier must be converted to binary numbers that is digestible by the PIC16F877A. Hence, the voltage divider network set with the resistance values of R_1=90KΩ and R_2=24KΩ.

9) Current sensing circuit: The operation amplifier LM358N with current sensing surface mount resistor of 0.1Ω with 10 W chosen for the current sensing circuit.

10) DC Motor: A 12 V DC motor is chosen for driving the pump.

11) Pump: a centrifugal pump may be used for pumping the water.

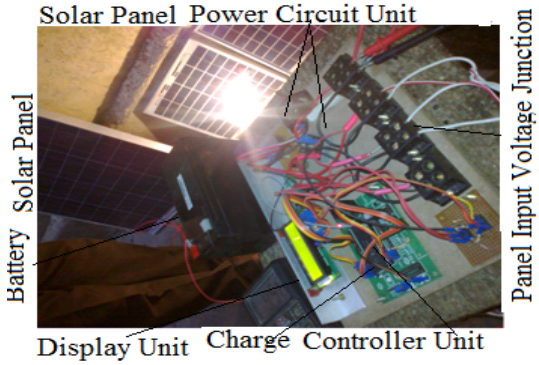

Fig.10. Snapshot of the Experimental setup showing the fabricated closed loop buck converter with MPPT algorithm.

The fabricated closed loop buck converter with MPPT algorithm is shown in fig.10.

The MPPT algorithm embedded in mikroC PRO software window for PIC microcontroller 16F877A is shown in fig.11.

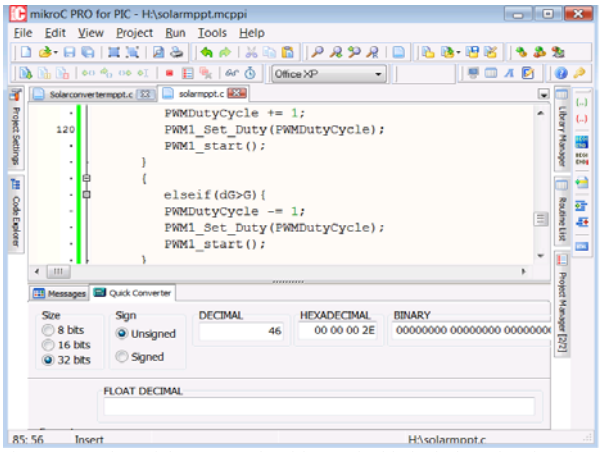

Fig.11. Snapshot of the MPPT algorithm embedded window showing the mikroC PRO software for PIC 16F877A microcontroller.

Fig.12. Snapshot of the Experimental setup showing the fabricated closed loop buck converter with MPPT algorithm and DC Motor for water pumping application.

Fig.12. shows the Snapshot of the Experimental setup for the fabricated closed loop buck converter with MPPT algorithm and DC Motor for water pumping application.

The driving gate pulse for buck converter across the MOSFET switch is shown in Fig.13.

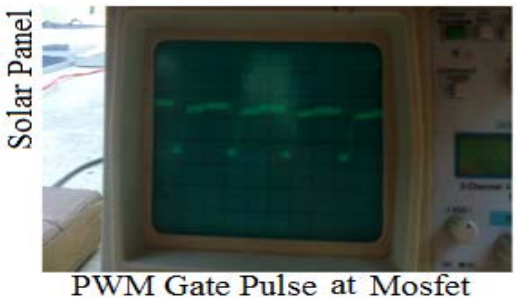

Fig.13. Snapshot showing the driving gate pulse across the MOSFET switch for Buck converter.

Fig.14. shows the input voltage to the buck converter from photovoltaic panel. Fig.15. shows the regulated output voltage (V_o) from the charge controller which can be used for driving the pump for water pumping application with MPPT algorithm.

Fig.14. Photocopy of the Experimental setup showing input voltage (V_{in}) of 18 V from the photovoltaic panel under 1000w/m^2 irradiation.

Fig.15. Photocopy of the Experimental setup showing output voltage (V_o) of 12 V from the charge controller under 1000w/m^2 irradiation.

The theoretical calculation of the amount of water that can be pumped by the rated 80 Watt Photovoltaic panel is given in Table II by assuming 80% of efficiency for all and four hours of illumination per day.

TABLE II

PV Panel (w)	Buck Converter (w)	DC Motor (w)	Centrifugal Pump (w)	Water Lifted in Liters/day	Head (m)
64	51.2	40.96	32.768	4810	10

VI. PARTIALLY SHADED CONDITION

In the new trend of integrated PV arrays, it is difficult to avoid partial shading of array due to neighboring buildings throughout the day in all the seasons. This makes the study of partial shading of module a key issue.

Partial shading of a solar photovoltaic module (SPM) is one of the main causes of overheating of shaded cells and reduced energy yield of the module with a physical solar PV module it is difficult to study the effects of partial shading.

MATLAB/Simulink model of a PV module consisting of 36 series has been developed to carry out this study. The model is used to study the effect of shade on varying number of cells on the power output of the module and stress on the shaded illuminated cells under various illumination levels. Fig.16 shows the Simulated Power curve for varying shade from 200 to 1000w/m^2.

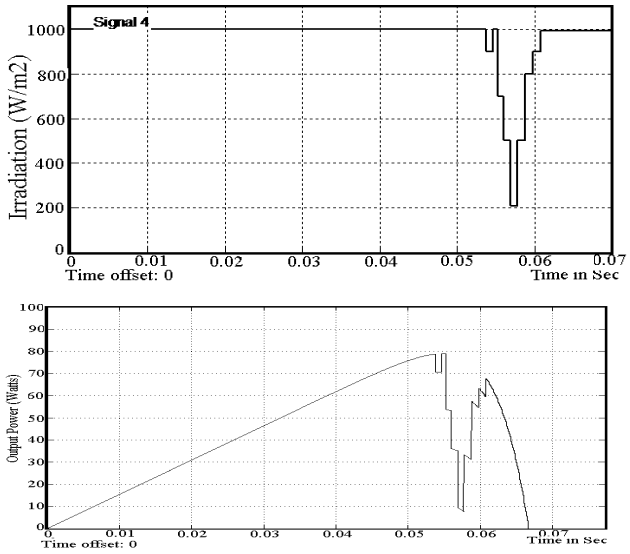

Fig.16. Simulated Power curve for varying shade from 200 to 1000w/m^2.

VII. CONCLUSION

The hardware and software analysis of the photovoltaic system with integrated MPP Tracker is presented in this paper. The simulation results show that the Incremental Conductance algorithm has the merits such as simplicity fast response, low over-tuning, high control, precision and easy implementation. The hardware results are in line with simulated results.

REFERENCES

[1] Bimal K. Bose, "Global Warming Energy: Environmental Pollution and the Impact of Power Electronics", IEEE Industrial Electronics Magazine, pp.1-17, March 2010.

[2] Adel Mellit, "Artificial Intelligence technique for modelling and forecasting of solar radiation data: a review," Int. J. Artificial Intelligence and Soft Computing Vol. 1. No. 1, 2008.

[3] Akihiro Oi, "Design and Simulation of Photovoltaic Water Pumping System", *Master of Science Thesis, California Polytechnic State University,* 2005.

[4] Adedamola Omole, "Analysis, Modelling and Simulation of Optimal Power Tracking of Multiple-Modules of Paralleled Solar Cell Systems", *Master of Science Thesis, The Florida State University College of Engineering*, 2006.

[5] V. Di Dio, D. La Cascia, R. Miceli, "A Mathematical Model to Determine the Electrical Energy Production in Photovoltaic Fields under Mismatch Effect", *Proceedings of the 978(1) IEEE,* pp.46-51, August 2009.

[6] Vaigundamoorthi.M and Ramesh.R, "Experimental Investigation of Chaos in Input Regulated Solar PV Powered" International Journal of Computer Applications (0975 – 8887) Volume 43– No.10, April 2012.

[7] Christopher A. Otieno, George N. Nyakoe, Cyrus W. Wekesa, "A Neural Fuzzy Based Maximum Power Point Tracker for a Photovoltaic System", *IEEE AFRICON*, September 23-25, pp.1-6, 2009.

[8] A. Mellit, "An ANFIS-Based Prediction for Monthly Clearness Index and Daily Solar Radiation: Application for sizing of a Stand-Alone Photovoltaic System", *Journal of Physical Science, Vol. 18(2),* pp.15–35, 2007.

[9] N. Patcharaprakiti and S. Premrudeepreechacharn, "Maximum PowerPoint Tracking Using Adaptive Fuzzy Logic Control for Gridconnected Photovoltaic System", PESW2002, volume 1, PP:372-377, 002.

[10] Marcelo Gradella Villalva, Jonas Rafael Gazoli, and Ernesto Ruppert Filho , "Comprehensive Approach to Modeling and Simulation of Photovoltaic Arrays", IEEE Transactions on Power Electronics, vol 24, no. 5, 2009, pp 1198-1208.

[11] A. Durgadevi, "Design of intelligent controller for quasi resonant converters", M.E. dissertation, Departmne of Electronics and Instrumentation Engineering, Annamalai Univ., Chidambaram, 2008.

[12] Vaigundamoorthi.M and Ramesh.R, "ZVS-PWM Active clamping modified cuk converter based MPPT for solar PV modules "European Journal of Scientific Research, Vol.58 No.3 (2011), pp.305-315.

[13] H. Yamashita and K. Tamahashi, et al, "A Novel Simulation Technique of the PV Generation System Using Real Weather Conditions," in Proceedings of the PCC,2002, volume2, PP:839-844, 2002

[14] Cung-Yuen Won, Duk-Heon Kim, Sei-chan Kim, Won-Sam Kim, hack_Sung Kim, "A New Maximum Power Point Tracker of Photovoltaic Arrays Using Fuzzy Controller", PESC'94.

[15] Guohui Zeng, Qizhong Liu, "An Intelligent Fuzzy Method for MPPT of Photovoltaic arrays", 2009 Second International Symposium on Computational Intelligence and Design, pp. 356-359.

[16] Rosaidi Bin Rosalan,"Maximum Power Point Tracking Converter for Photovoltaic Application", B.E. dissertaion, Faculty of Electrical Engineering, Universiti Teknologi Malaysia, 2009.